Available online at www.sciencedirect.com
ScienceDirect
Journal of Magnetic Resonance 188 (2007) 337–343
JMR Journal of Magnetic Resonance
www.elsevier.com/locate/jmr

# On Cu(II)–Cu(II) distance measurements using pulsed electron electron double resonance

Zhongyu Yang, James Becker, Sunil Saxena *

*Department of Chemistry, University of Pittsburgh, Pittsburgh, PA 15260, USA*

Received 16 March 2007; revised 10 August 2007
Available online 16 August 2007

**Abstract**

The effects of orientational selectivity on the 4-pulse electron electron double resonance (PELDOR) ESR spectra of coupled Cu(II)–Cu(II) spins are presented. The data were collected at four magnetic fields on a poly-proline peptide containing two Cu(II) centers. The Cu(II)–PELDOR spectra of this peptide do not change appreciably with magnetic field at X-band. The data were analyzed by adapting the theory of Maryasov, Tsvetkov, and Raap [A.G. Maryasov, Y.D. Tsvetkov, J. Raap, Weakly coupled radical pairs in solids:ELDOR in ESE structure studies, Appl. Magn. Reson. 14 (1998) 101–113]. Simulations indicate that orientational effects are important for Cu(II)–PELDOR. Based on simulations, the field-independence of the PELDOR data for this peptide is likely due to two effects. First, for this peptide, the Cu(II) *g*-tensor(s) are in a very specific orientation with respect to the interspin vector. Second, the flexibility of the peptide washes out the orientation effects. These effects reduce the suitability of the poly-proline based peptide as a good model system to experimentally probe orientational effects in such experiments. An average Cu(II)–Cu(II) distance of 2.1–2.2 nm was determined, which is consistent with earlier double quantum coherence ESR results.


*Keywords:* Dipolar interaction; Pulsed electron electron double resonance; Distance determination; Cu(II)–Cu(II) distances; ESR

## 1. Introduction

The sensitivity of pulsed electron spin resonance (ESR) to magnetic dipolar interactions has recently provided a powerful methodology to measure the distance (~18–70 Å) between two spin labels [1–7], in order to establish global folding patterns in proteins [8–14] and nucleic acids [15–18]. Thus far, the ESR method has largely been restricted to the use of nitroxide as the spin labels. The internal orientation of the nitroxide spin labels typically have only a small effect on the spectral line shape in the pulsed electron electron double resonance (PELDOR) at X-band [2], although they have been observed in some cases [19]. These orientation effects become significant at higher frequencies [20,21], and can be used to infer the relative orientation of the spin labels.

Recently, the ESR distance mapping methodology has been extended to the case of paramagnetic metal centers in metalloproteins [22–24], oligomers [25], and peptides [26]. For paramagnetic metals, the large *g* and hyperfine anisotropies can complicate the analysis of the experimental spectra. There is limited information about the effect of the internal orientation on the Cu(II)–Cu(II) distance measurements using PELDOR. Previous papers on Cu(II)–Cu(II) distance measurements using pulsed ESR only focused on the $g_\perp$ range of the Cu(II)–ESR spectrum [22,23,26].

In this paper, we address the effects of orientational selectivity in the 4-pulse PELDOR spectra of Cu(II) spins. Experimental data were obtained using a model peptide that contains Cu(II) binding sites [26]. The effects of internal orientation on the Cu(II)–Cu(II) distance are analyzed by using the theory of Maryasov et al. [27]. By fitting the experimental data to the theory, the Cu(II)–Cu(II) distance is determined. The results indicate that, for this peptide, the

* Corresponding author. Fax: +1 412 624 8611.
*E-mail address:* sksaxena@pitt.edu (S. Saxena).

1090-7807/$ - see front matter © 2007 Elsevier Inc. All rights reserved.
doi:10.1016/j.jmr.2007.08.006

PELDOR line shape does not depend on the magnetic field at X-band. However, in general, the effects of the orientational selectivity must be considered so that accurate distance constraints are measured.

## 2. Results and discussion

A poly-proline peptide, shown in Fig. 1a, with a sequence of PHGGGP$_3$HGGGW with two Cu(II) binding PHGGGW sequence was used for the experiments [28]. Fig. 1b shows the field-swept echo-detected ESR signal from the poly-proline peptide, obtained using a $\pi/2$–$\tau$–$\pi$ sequence [29]. The line shape is characteristic of an axially symmetric $g$-tensor (electron spin-1/2) with hyperfine splitting from the nuclei of spin-3/2. These splittings are evident for the larger $A_\parallel$ component and are shown by arrows in Fig. 1b. Each "resonance-field" in the spectrum consists of contribution from an orientation (or from a set of orientations) of the magnetic field with respect to the principal axis system (PAS) of the $g$-tensor for each Cu(II) center (cf. inset to Fig. 1b for definition of angles). To first order, and given that the electron electron dipolar (EED) interaction is weak, the resonance field, $B_{\text{res}}$, for an orientation $\beta_i$ ($i = 1, 2$, cf. Fig. 1b) is given by [30]

$$B_{\text{res}} = \frac{h\nu_0}{g_{\beta_i}\beta_e} - A_{\beta_i} m_I \tag{1}$$

where $m_I$ is the nuclear spin quantum number, $\nu_0$ is the spectrometer frequency, $\beta_e$ is Bohr magnetron for electrons, and $g_{\beta_i}$, and $A_{\beta_i}$ are defined as

$$g_{\beta_i} = \left[g_\perp^2 \sin^2\beta_i + g_\parallel^2 \cos^2\beta_i\right]^{1/2}$$

and

$$A_{\beta_i} = \left[\frac{(A_\parallel^2 g_\parallel^2 - A_\perp^2 g_\perp^2)\cos^2\beta_i + A_\perp^2 g_\perp^2}{g_{\beta_i}^2}\right]^{1/2} \tag{2}$$

where $g_\parallel$, $g_\perp$, $A_\parallel$, and $A_\perp$ are the parallel and perpendicular components of the $g$- and hyperfine tensors, respectively. A spectrum simulated using Eqs. (1) and (2) and with $g_\parallel$, $g_\perp$, $A_\parallel$, and $A_\perp$ of 2.230, 2.068, 165.0, and 2.0 G, respectively, is shown in Fig. 1b.

The value of the hyperfine splitting is characteristic of Cu(II) coordinated to three nitrogen atoms and one oxygen atom [28,31]. This was confirmed by electron spin echo envelope modulation (ESEEM) experiments [26] which contain peaks due to electron nuclear dipolar (END) interactions with the remote $^{14}$N nuclear spin of the imidazole and with the $^{14}$N nuclear spin of the non-coordinated glycine residue [32].

Fig. 2 shows the time domain PELDOR signal for the poly-proline peptide at four different magnetic fields. In this two frequency experiment [1,3], the detection frequency was 9.556 GHz and the pump frequency was 9.656 GHz. The separation between the detection pulse and the pump pulse was extended to 100 MHz, in order to reduce the ESEEM effect [2]. In the experiments, the modulation depth depended on the magnetic field and ranged from 0.6% to 1%. The modulation depth calculated from theory is 1–2.5% [1]. The intramolecular dipolar modulation between the two Cu(II) spins is evident in the range of ~200 ns. The decay of the time domain trace is due to the intermolecular dipolar interaction between the Cu(II) electron spins. The total time domain signal can be expressed as [33,34]

$$V(t)_{\text{total}} = V(t)_{\text{inter}} V(t)_{\text{intra}} \tag{3}$$

The intramolecular time domain signal at each magnetic field was obtained after a baseline correction and the resultant intramolecular time traces are shown in Fig. 3a. The Fourier transform of the intramolecular time domain traces is shown in Fig. 3b at the four different magnetic fields. The PELDOR signal monitors the modulation due to the EED interaction which occurs at a frequency of [35]

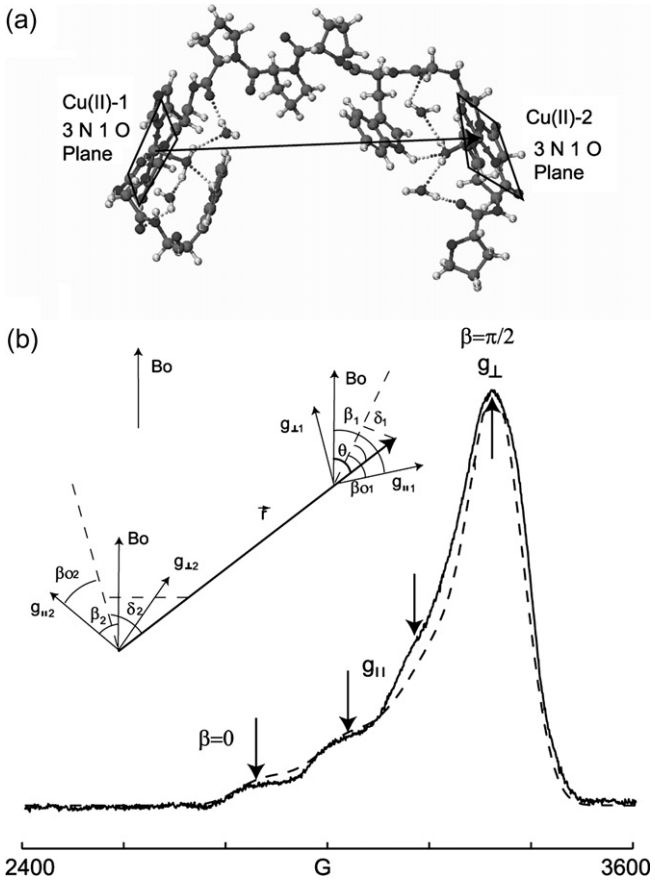


Fig. 1. (a) The modeled structure of the Cu(II) binding peptide is shown [26]. The dipolar vector forms an angle of close to 90° with respect to the Cu(II) binding ligand plane (shown by rectangles). (b) Field-swept electron spin echo detected Cu(II)–ESR spectrum of the peptide at 20 K with a simulated spectrum shown as the dashed line. The principal axis system (PAS) with respect to the magnetic field and interspin vector is shown in the inset. Each spectral position corresponds to an orientation, $\beta$ (or a set of orientations), of the PAS with respect to the magnetic field. The data are consistent with Cu(II) binding to the PHGGGW sequence [32]. Arrows show the larger hyperfine splitting.

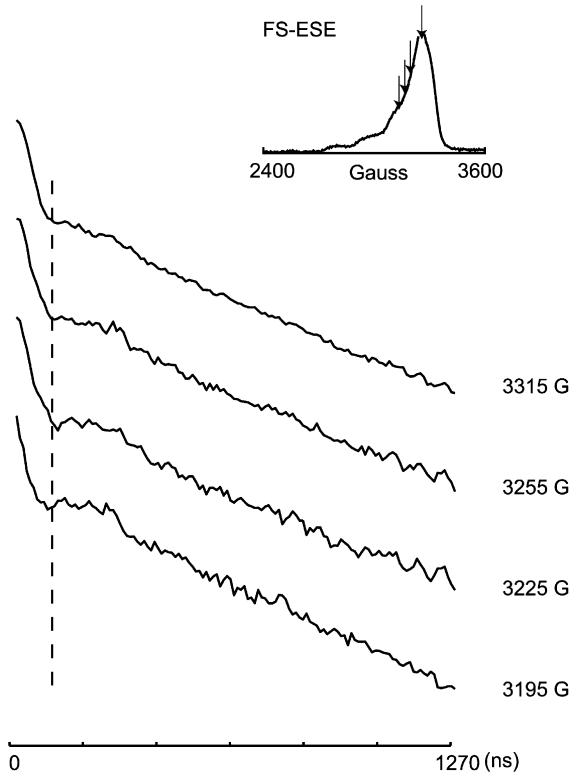


Fig. 2. Time domain data of the Cu(II)–PELDOR spectra. The magnetic fields used are shown by arrows on the FS-ESE spectrum, shown in the inset. The fast modulation in the time domain is from proton-ESEEM.

$$\upsilon_d = \frac{\mu_0 g_a g_b \beta_e^2}{4\pi h r^3}\left(3\cos^2\theta - 1\right) \tag{4}$$

where $\mu_0$ is the permeability of free space, $g_{a,b}$ are the $g$-factors for the electrons, $r_{ab}$ is the Cu(II)–Cu(II) distance, and $\theta$ is the angle between the interelectron vector and the static magnetic field (cf. Fig. 1b, inset).

In general, the large anisotropy in the $g$-tensor can present an interesting opportunity for the case of Cu(II)–ESR. The experiment was obtained with detection pulses of 24 ns ($\pi/2$ pulse) and 48 ns ($\pi$ pulse) and a pump pulse of 48 ns ($\pi$ pulse). At a given magnetic field, the pulses "reorient" spin packets that are within a narrow bandwidth of about 41 MHz, compared to the full spectral bandwidth of ~2 GHz. Therefore, at a given magnetic field, only a subset of orientations of PAS (given by angles $\delta_i$, $\beta_i$), and, therefore, $\theta$ angles, are excited by the selective microwave pulses. From Fig. 1b inset, it follows that

$$\cos\theta_i = \cos\delta_i \cos(\beta_i - \beta_{0i}), \quad i = 1,2 \tag{5}$$

As shown in Fig. 1b inset, for the $i$th Cu(II) spin, $\beta_i$ is the angle between the $g_\parallel$ and the external magnetic field, Bo. $\theta$ is the angle between the interspin vector and the external magnetic field, Bo. The projection of the interspin vector on the $g_\parallel$ and $g_\perp$ plane forms an angle of $\beta_{0i}$ with respect to the $g_\parallel$ axis. The angle between the interspin vector and its projection on the $g_\parallel$ and $g_\perp$ plane is defined by $\delta_i$.

From Eqs. (1)–(5), it follows that the PELDOR frequency should vary with magnetic field in a fashion that depends on the angles $\delta_i$ and $\beta_{0i}$. However, the PELDOR data on the poly-proline peptide do not vary with magnetic fields (cf. Fig. 2). The peak frequency is ~3.9 MHz.

In order to quantitatively analyze this effect, we use the theory of Maryasov, Tsvetkov, and Raap [27]. The PELDOR signal, $V(T)$, is given by [27]

$$V(T) = \int_0^1 \xi(\cos\theta)\left\langle 1 - \cos\left\{[\omega_D(1 - 3\cos^2\theta) + J]T\right\}\right\rangle \mathrm{d}\cos\theta \tag{6}$$

where the function $\xi(\cos\theta)$ contains information about the orientation of the spins and was called the geometrical factor. The geometrical factor is given by [27]

$$\xi(\cos\theta) = \frac{1}{2}\sum_{m_{I1},m_{I2}} \left\langle k_{xa}^3 k_{xb}^2 \sin\phi_{1a}(1-\cos\phi_{2a})(1-\cos\phi_{3b}) + k_{xb}^3 k_{xa}^2 \sin\phi_{1b}(1-\cos\phi_{2b})(1-\cos\phi_{3a})\right\rangle_{\Phi,\delta\omega_1,\delta\omega_2}$$

where

$$k_{xq} = B_{lq}/B_{rq} \tag{7}$$

and

$$B_{rq} = \left([(\omega_{rq} - \omega_q)/\gamma^2]^2 + B_{lq}^2\right)^{\frac{1}{2}} \tag{8}$$

in which $\omega_a$ and $\omega_b$ are the frequencies of the detection pulse and the pump pulse, respectively. $B_{lq}$ is the amplitude of oscillating magnetic field at frequency $\omega_q$, where $q = a, b$; $\omega_{rq}$ is the resonance frequency; Eq. (8) includes the effect of inhomogeneous broadening of the ESR lines [3]; $\gamma$ is the gyromagnetic ratio for the electron; $\phi_{1a}$, $\phi_{2a}$, and $\phi_{3b}$ are the rotation angles of the $i$th pulse. These rotation angles are expressed as [27]

$$\phi_{iq} = \gamma B_{rq} t_{pi} \tag{9}$$

If all orientations are excited, as is substantially the case for nitroxides [27], the orientation factor is practically uniform for all values of $\cos(\theta)$ and a characteristic Pake pattern results [36]. In the Pake pattern, the frequency corresponding to $\theta = 90°$ dominates (cf. Eq. (4)), due to the greater probability of the presence of molecules with $\theta = 90°$ in the powder sample.

The presence of finite pulse-lengths, and large $g$- and hyperfine anisotropies, as in Cu(II) can lead to large orientation effects. Fig. 4a and b shows the simulated geometrical factor, $\xi(\cos\theta)$ and PELDOR spectrum, based on Eqs. (6) and (7), respectively. In these simulations, a single Cu(II)–Cu(II) distance is selected as 2.2 nm. The orientations of the principal axis systems for the two Cu(II) centers were set at $\beta_{01} = \beta_{02} = 0°$, $\delta_1 = \delta_2 = 0°$. $\delta_i$ was chosen as 0° since in this case the orientational selectivity of the PELDOR spectrum is the maximum. Only $\beta_{0i}$ values of 0° are shown in Fig. 4. Similar results were obtained with other $\beta_{0i}$ values. At the magnetic field of 2900 G, the simulated DEER spectrum consists of single peak at 4.1 MHz. Non-selective excitation would have yielded a Pake pattern with a dominant $\theta = 90°$ peak of 4.8 MHz (from Eq. (4) with $\theta = 90°$ and

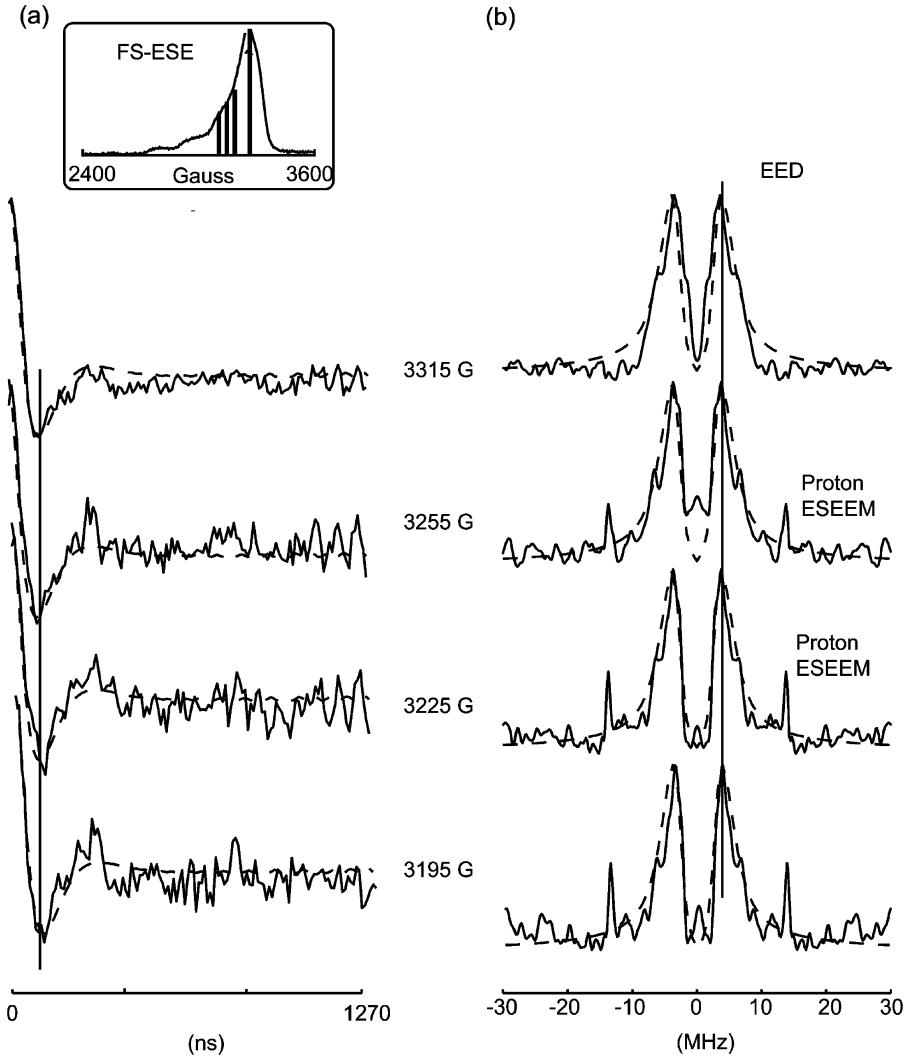


Fig. 3. (a) The time domain signal of the Cu(II)–PELDOR after baseline correction. The position of magnetic fields need is shown on the field swept Cu(II)–ESE spectrum in the inset. The period of the dipolar modulation of the time domain is similar at each magnetic field. (b) The Fourier transformation of the baseline corrected time domain signal. At each magnetic field, the dominant frequency peak appears at ~3.9 MHz. The 14.8 MHz peak is from proton-ESEEM.

$r = 2.2$ nm). The results can be rationalized from the geometrical factor, $\xi(\cos\theta)$. At this magnetic field and with $\beta_{01} = \beta_{02} = \delta_1 = \delta_2 = 0.0°$, the geometrical factor peaks at $\theta \sim 38°$ (cf. Fig. 4a and b), which from Eq. (4) leads to a frequency ~4.1 MHz in the DEER spectrum.

Fig. 4c and d illustrates the orientational selectivity imparted by the choice of magnetic fields. At a magnetic field of 3000 G, the geometrical function is bimodal with peaks at $\theta \sim 30°$ and at $\theta \sim 53°$ which leads to frequencies of 6.1, 0.4 MHz in Eq. (4). The simulated DEER spectrum based on Eq. (7) yields peaks at 6.1 and 0.4 MHz. At 3100 G magnetic field, orientations with $\theta \sim 10°$, 51°, and 68° are predominantly excited, which corresponds to frequencies of 9.3, 0.9, and 2.8 MHz. From the simulated Pake pattern, the same frequency peaks were obtained. Finally, at 3200 G orientation with $\theta$ centered at 50°, 73°, and 80° are excited. The distribution between 73° and 80° generates a broad peak around 4.8 MHz while a peak at 0.9 MHz results from excitation of $\theta \sim 50°$. Therefore, theoretically, when $\delta \sim 0°$, there is strong orientational selectivity on the Cu(II)–PELDOR spectra, at X-band. Different DEER spectra are anticipated at different magnetic field.

The magnetic field dependence of PELDOR frequency persists even in the presence of a distribution in distances. Fig. 5 shows simulated PELDOR spectra, based on Eq. (6) for different values of the magnetic field in the presence of a distribution of distances. A Gaussian distribution function with a mean distance of 2.2 nm and a standard deviation of 0.3 nm was used. The orientations were held at $\beta_{01} = \beta_{02} = 135°$, $\delta_1 = \delta_2 = 0°$. The PELDOR spectrum changes with magnetic field and the prominent frequency changes from 1.4 to 4.1 MHz. However, this effect will be subtle in the presence of noise.

The results indicate that the presence of substantial $g$ and hyperfine anisotropies leads to the excitation of only certain orientation at a given magnetic field when $\delta_i \sim 0°$.

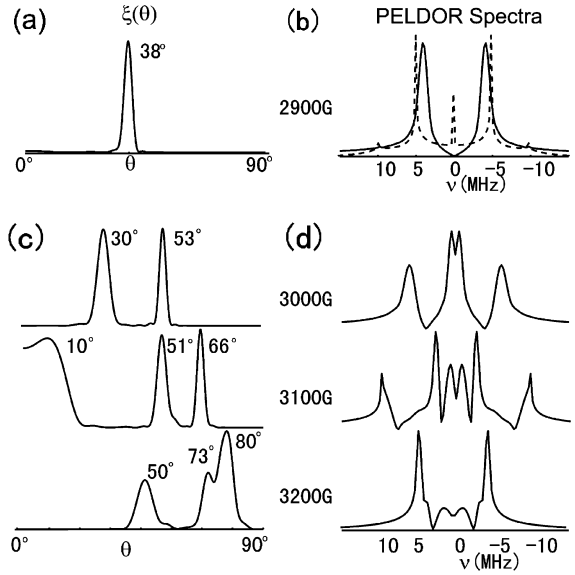


Fig. 4. (a) The geometrical factor calculated using Eq. (6) for $\beta_{01} = \beta_{02} = 0°$, $\delta_1 = \delta_2 = 0°$, $r = 2.2$ nm, and $B_0 = 2900$ G is shown. The plot indicates that at this magnetic field and for these parameters, only $\theta \sim 38°$ orientations are excited by the selective pulse. (b) The simulated PELDOR spectrum consequently yields a frequency of 4.1 MHz (solid line). Non-selective excitation would yield a Pake pattern with a dominant peak at 4.8 MHz (dashed line). (c) The simulated geometrical factor with the same parameters but at three different magnetic fields is shown. These results indicate that the $\theta$ angles are different at different magnetic field. Therefore, the resultant PELDOR spectrum varies with magnetic field. (d) The simulated PELDOR spectra based on Eq. (7) at three magnetic fields are shown. Such orientational effects are reduced when $\delta_1 \sim 90°$ and $\delta_2 \sim 90°$.

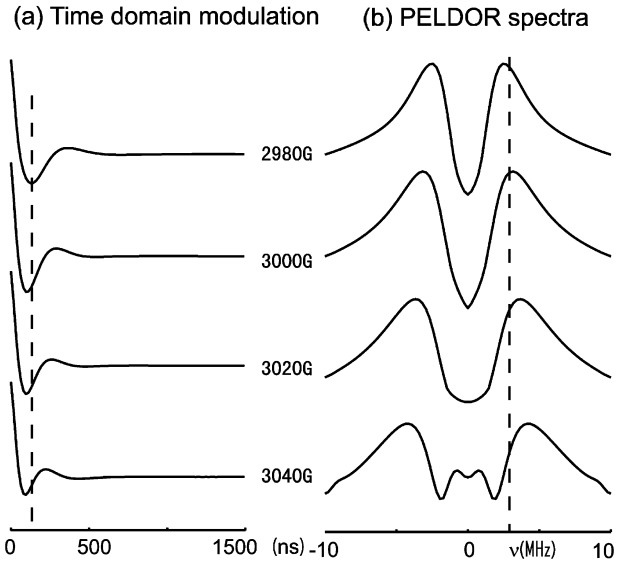


Fig. 5. The magnetic field dependence of PELDOR frequency persists even in the presence of a distribution in distances. (a) Simulated time domain signal and (b) the spectra at 2980, 3000, 3020, and 3040 G, with $\beta_{01} = \beta_{02} = 135°$, $\delta_1 = \delta_2 = 0°$. The interspin distance is held at 2.2 nm and a standard Gaussian distance distribution is used as 0.3 nm. The frequency shifts from 1.4 to 4.1 MHz. Such orientational effects are reduced when $\delta_1 \sim 90°$ and $\delta_2 \sim 90°$.

The PELDOR spectrum deviates from a simple Pake pattern and should vary with different magnetic field.

However, the orientational selectivity is washed out when $\delta_i$ approaches to 90°, as is evident from Eq. (5). Under this condition, only the orientation with $\theta \sim 90°$ are excited, and these features dominate the PELDOR spectrum (simulation data not shown).

The field-independence of experimental data (shown in Figs. 2 and 3) is possibly due to the combination of two effects. First, the orientation effects of Cu(II) electron spin are washed out by the flexibility of the peptide, which yields a large distribution in Cu(II)–Cu(II) distances. Second, for this poly-proline peptide the Cu(II) $\delta_1$ and $\delta_2$ may be close to 90°. The modeled structure of the Cu(II) binding peptide is shown in Fig. 1a [26]. The dipolar vector forms an angle of close to 90° with respect to the Cu(II) binding ligand plane. The angles between the Cu(II)–Cu(II) dipolar vector and each Cu(II) binding ligand (3 N 1 O) for the first Cu(II) are 82°, 118°, 92°, and 84°. The angles between the Cu(II)–Cu(II) dipolar vector and each Cu(II) binding ligand (3 N 1 O) for the second Cu(II) are 110°, 81°, 75°, and 106°. Therefore, the dipolar vector could form an angle of close to 90° with respect to the Cu(II) $g$-tensor plane. With the internal orientation that $\delta_1$ and $\delta_2 \sim 90°$, the best fits were obtained with a Gaussian distribution of distances with an average interspin distance of 2.1–2.2 nm and a standard deviation of 0.3 nm. Similar results were obtained for any $\beta_{0i}$ value. The resulted time traces and PELDOR spectra are shown by dashed line in Fig. 3. Double quantum coherence ESR results measured a distance of 2.0 nm on the same peptide [26]. The $\delta_i$ values estimated from this work are consistent with the assumption made by Huber and coworkers in their metalloprotein [23].

Large distance measurements on spin-labeled macromolecules have opened up the use of ESR to measure global folding patterns of proteins, nucleic acids, and flexibility of polymers. Extension of this methodology to paramagnetic metals is likely to have a similar impact on the measurement of structure–function relationships in metalloproteins.

## 3. Conclusions

In this work, we present the Cu(II)–PELDOR spectra at four magnetic fields, at X-band. We found that the Cu(II)–PELDOR spectra do not vary with magnetic field. However, theory predicts that the Cu(II)–PELDOR spectra should vary with magnetic field. We explained this magnetic field independency by the combination of two possible effects. First, the flexibility of the model peptide washes out the orientational selectivity of the Cu(II)–PELDOR spectra. Second, the Cu(II) $g$-tensor in our model peptide is in a specific orientation with respect to the interspin vector (cf. Fig. 1a)—at these orientations the PELDOR data are expected to be field independent from theory. The combination of large flexibility and mutual orientations reduces the suitability of poly-proline based systems to monitor orientational effects in these experiments.

However, the simulations indicate that, in general, the orientation effects are important for obtaining accurate Cu(II)–Cu(II) distance using PELDOR, and field dependent data should be acquired and analyzed as discussed in this work.

## Materials, experiments, and analysis procedures

A peptide with a sequence of $PHGGGWP_3HGGGW$ was synthesized. The PHGGGW sequence is a common copper binding motif found in the prion protein [32]. For ESR experiments, a 3.5 mM solution of the peptide in 30% glycerol/30% 2,2,2-trifluoroethanol/40% water containing 150 mM NaCl, buffered to pH 7.46 using *N*-ethylmorpholine was prepared. Two equivalents of Cu(II) were added to the solution from a 0.1 M standard solution of $CuSO_4$. About 30 μl of this solution was used for ESR experiments. All experiments were performed at a temperature of 20 K on a Bruker ElexSys E580 CW/FT ESR spectrometer. For the 4-pulse PELDOR experiments, a $(\pi/2)_{v1} - \tau_1 - (\pi)_{v1} - (\tau_1 + T) - (\pi)_{v2} - (\tau_2 - T) - (\pi)_{v2}$ pulse sequence was used. The detection pulse length was 24 ns and its frequency ($v_1$) was 9.556 GHz. The pump pulse length was 48 ns and its frequency ($v_2$) was 9.656 GHz. These pulse-lengths were chosen to minimize the proton and Nitrogen-14 ESEEM in this system [28].

The pulse separations, $\tau_1$, $\tau_2$, were 200 and 1400 ns, respectively, and the echo signal was integrated using a video amplifier bandwidth of 20 MHz. The pump pulse was stepped out by 10 ns for a total of 128 points in $T$. In order to reduce the proton-ESEEM, the $\tau_1$ separation was also stepped out by 16 ns (which is 25% of the proton-ESEEM modulation period) for a total of four data points [37], the final PELDOR signal was summed up from the signal at each of the four $\tau_1$ values. The $T = 0$ value was carefully calibrated using a nitroxide biradical sample.

## Acknowledgments

This research was supported by an NSF-CAREER award (MCB 0346898). The help of Soraya Pornsuwan with initial data analysis is gratefully acknowledged.

## References

[1] A.D. Milov, A.B. Ponomarev, Y.D. Tsvetkov, Electron–electron double resonance in electron spin echo: model biradical systems and the sensitized photolysis of decalin, Chem. Phys. Lett. 110 (1984) 67–72.
[2] R.G. Larson, D.J. Singel, Double electron–electron resonance spin–echo modulation spectroscopic measurement of electron–spin pair separations in orientationally disordered solids, J. Chem. Phys. 98 (1993) 5134–5146.
[3] A.D. Milov, A.G. Maryasov, Y.D. Tsvetkov, Pulsed electron double resonance (PELDOR) and its applications in free-radicals research, Appl. Magn. Reson. 15 (1998) 107–143.
[4] M. Pannier, S. Veit, A. Godt, G. Jeschke, H. Spiess, Dead-time free measurement of dipole–dipole interactions between electron spins, J. Magn. Reson. 142 (2000) 331.
[5] S. Saxena, J. Freed, Theory of double quantum two-dimensional electron spin resonance with application to distance measurements, J. Chem. Phys. 107 (1997) 1317.
[6] P.P. Borbat, A.J. Costa-Filho, K.A. Earle, J.K. Moscicki, J.H. Freed, Electron spin resonance in studies of membranes and proteins, Science 291 (2001) 266–269.
[7] Y. Zhou, B.E. Bowler, K. Lynch, S.S. Eaton, G.R. Eaton, Interspin distances in spin-labeled Metmyoglobin variants determined by Saturation Recovery EPR, Biophys. J. 79 (2000) 1039–1052.
[8] P. Borbat, H. Mchaorab, J. Freed, Protein structure determination using long-distance constraints from double-quantum coherence ESR: study of T4 lysozyme, J. Am. Chem. Soc. 124 (2002) 5304–5314.
[9] M. Bennati, A. Weber, J. Antonic, D.L. Perlstein, J. Robblee, J. Stubbe, Pulsed ELDOR spectroscopy measures the distance between the two tyrosyl radicals in the R2 subunit of the *E. coli* Ribonucleotide Reductase, J. Am. Chem. Soc. 125 (2003) 14988–14989.
[10] G. Jeschke, C. Wegener, M. Nietschke, H. Jung, H.-J. Steinhoff, Interresidual distance determination by four-pulse Double Electron-Electron Resonance in an integral membrane protein: the $Na^+$/proline transporter PutP of *Escherichia coli*, Biophys. J. 86 (2004) 2551–2557.
[11] A. Kawamori, T.-A. Ono, A. Ishii, S. Nakazawa, H. Hara, T. Tomo, J. Minagawa, R. Bittl, S.A. Dzuba, The functional sites of chlorophylls in D1 and D2 subunits of Photosystem II identified by pulsed EPR, Photosynth. Res. 84 (2005) 187–192.
[12] M.J. Swamy, L. Ciani, M. Ge, A.K. Smith, D. Holowka, B. Baird, J.H. Freed, Coexisting domains in the plasma membranes of live cells characterized by spin-label ESR spectroscopy, Biophys. J. 90 (2006) 4452–4465.
[13] T. Aihara, S. Ueki, M. Nakamura, T. Arata, Calcium-dependent movement of troponin I between troponin C and actin as revealed by spin-labeling EPR, Biochem. Biophys. Res. Commun. 340 (2006) 462–468.
[14] Q. Xu, J.F. Ellena, M. Kim, D.S. Cafiso, Substrate-dependent unfolding of the energy coupling motif of a membrane transport protein determined by double electron–electron resonance, Biochemistry 45 (2006) 10847–10854.
[15] O. Schiemann, A. Weber, T. Edwards, T. Prisner, S. Sigurdsson, Nanometer distance measurements on RNA using PELDOR, J. Am. Chem. Soc. 125 (2003) 3434–3435.
[16] P.P. Borbat, J.H. Davis, S.E. Butcher, J.H. Freed, Measurement of large distances in biomolecules using double-quantum filtered refocused electron spin-echoes, J. Am. Chem. Soc. 126 (2004) 7746–7747.
[17] O. Schiemann, N. Piton, Y. Mu, G. Stock, J.W. Engels, T.F. Prisner, A PELDOR-based nanometer distance ruler for oligonucleotides, J. Am. Chem. Soc. 126 (2004) 5722–5729.
[18] N. Piton, O. Schiemann, Y. Mu, G. Stock, T. Prisner, J. Engels, Synthesis of spin-labeled rnas for long range distance measurements by PELDOR, nucleosides, Nucleotides Nucleic Acids 24 (2005) 771–775.
[19] A. Godt, M. Schulte, H. Zimmermann, G. Jeschke, How flexible are poly(para-phenyleneethynylene)s? Angew. Chem., Int. Ed. 45 (2006) 7560–7564.
[20] V.P. Denysenkov, T.F. Prisner, J. Stubbe, M. Bennati, High-field pulsed electron–electron double resonance spectroscopy to determine the orientation of the tyrosyl radicals in ribonucleotide reductase, Proc. Natl. Acad. Sci. USA 103 (2006) 13386–13390.
[21] Y. Polyhach, A. Godt, C. Bauer, G. Jeschke, Spin pair geometry revealed by high-field DEER in the presence of conformational distributions, J. Magn. Reson. 185 (2007) 118–129.
[22] C. Elsasser, M. Brecht, R. Bittl, Pulsed electron–electron double resonance on multinuclear metal clusters: assignment of spin projection factors based on the dipolar interaction, J. Am. Chem. Soc. 124 (2002) 12606–21611.
[23] I.M.C. vanAmsterdam, M. Ubbink, G.W. Canters, M. Huber, Measurement of a Cu–Cu distance of 26 Å by a pulsed EPR method, Angew. Chem., Int. Ed. 42 (2003) 62–64.

[24] A.V. Astashkin, J. Seravalli, S.O. Mansoorabadi, G.H. Reed, S.W. Ragsdale, Pulsed electron paramagnetic resonance experiments identify the paramagnetic intermediates in the pyruvate ferredoxin oxidoreductase catalytic cycle, J. Am. Chem. Soc. 128 (2006) 3888–3889.
[25] E. Narr, A. Godt, G. Jeschke, Selective measurements of a nitroxide–nitroxide separation of 5 nm and a nitroxide–copper separation of 2.5 nm in a terpyridine based copper(II) complex by pulse EPR spectroscopy, Angew. Chem., Int. Ed. 41 (2002) 3907–3910.
[26] J. Becker, S. Saxena, Double quantum coherence electron spin resonance on coupled Cu(II)–Cu(II) electron spins, Chem. Phys. Lett. 414 (2005) 248.
[27] A.G. Maryasov, Y.D. Tsvetkov, J. Raap, Weakly coupled radical pairs in solids:ELDOR in ESE structure studies, Appl. Magn. Reson. 14 (1998) 101–113.
[28] E. Aronoff-Spencer, C.S. Burns, N.I. Avdievich, G.J. Gerfen, J. Peisach, W.E. Antholine, H.L. Ball, F.E. Cohen, S.B. Prusiner, G.L. Millhauser, Identification of the Cu(II) binding sites in the N-terminal domain of the prion protein by EPR and CD spectroscopy, Biochemistry 39 (2000) 13760–13771.
[29] A. Schweiger, G. Jeschke, Principles of Pulse Electron Paramagnetic Resonance, Oxford University Press, Oxford, 2001.
[30] C.P. Poole, Electron Spin Resonance: A Comprehensive Treatise on Experimental Technique, John Wiley & Sons, Inc., Toronto, 1983.
[31] J. Peisach, W.E. Blumberg, Structural implications derived from the analysis of Electron Paramagnetic Resonance spectra of natural and artificial copper proteins, Arch. Biochem. Biophys. 165 (1974) 691–708.
[32] C. Burns, E. Aronoff-Spencer, C. Dunham, P. Lario, N. Avdievich, W. Antholine, M. Olmstead, A. Vrielink, G. Gerfen, J. Peisach, W. Scott, G. Millhauser, Molecular features of the copper binding sites in the octarepeat domain of the prion protein, Biochemistry 41 (2002) 3991–4001.
[33] A.D. Milov, Y.D. Tsvetkov, F. Formaggio, M. Crisma, C. Toniolo, J. Raap, The secondary structure of a membrane-modifying peptide in a supramolecular assembly studied by PELDOR and CW-ESR spectroscopies, J. Am. Chem. Soc. 123 (2001) 3784–3789.
[34] C.G. Wong, T. Bottiglieri, O.C. Snead third, GABA, gamma-hydroxybutyric acid, and neurological disease, Ann. Neurol. 54 (Suppl. 6) (2003) S3–S12.
[35] L.J. Berliner, S.S. Eaton, G.R. Eaton, Biological Magnetic Resonance, Kluwer Academic/Plenum Publisher, New York, 2000.
[36] G.E. Pake, Nuclear resonance absorption in hydrated crystals: fine structure of the proton line, J. Chem. Phys. 16 (1948) 326–327.
[37] G. Jeschke, M. Pannier, A. Godt, H. Spiess, Dipolar spectroscopy and spin alignment in electron paramagnetic resonance, Chem. Phys. Lett. 331 (2000) 243–252.